

# Triboelectric Nanogenerator Array as a Probe for In Situ Dynamic Mapping of Interface Charge Transfer at a Liquid–Solid Contacting

Jinyang Zhang,<sup>#</sup> Shiquan Lin,<sup>#</sup> and Zhong Lin Wang<sup>\*</sup>



Cite This: <https://doi.org/10.1021/acsnano.2c11633>



Read Online

ACCESS |



Metrics & More



Article Recommendations



Supporting Information

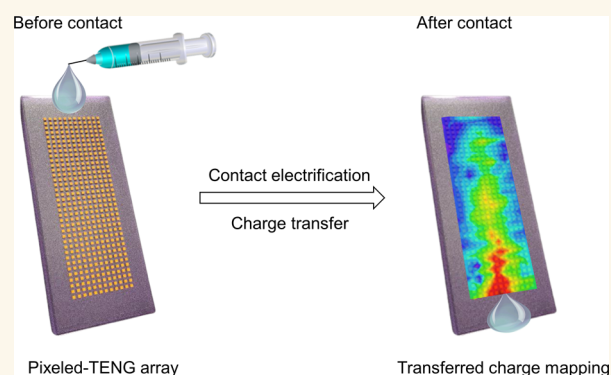
**ABSTRACT:** Contact between water droplets with hydrophobic surfaces is a common phenomenon at functional interfaces, and it has been extensively studied. However, quantifying the charge transfer between the liquid–solid interfacial contacting, especially for the charge density distribution throughout the movement of liquid droplet on a dielectric surface, remains to be investigated. Here, we developed a pixelated droplet triboelectric nanogenerator (pixelated droplet-TENG) array with high-density electrode array as a probe for measuring the charge transfer at a liquid–solid interface when a water drop moves on the hydrophobic surface. To intuitively observe the charge transfer between the liquid–solid interface, we “imaged” the transferred charges along movement trajectory of a water droplet as it slides along a tilted solid surface at a spatial resolution of 0.4 mm and time sensitivity of 0.02 s. Our study shows that the transferred charges are not uniformly distributed along the path, which is possibly due to the two-step model of electron transfer and ion adsorbed on the solid surface, and thus the formation of an electric double layer will inevitably shield the net surface on the solid surface. Our study presents a probe technology with potential applications in surface chemistry, physics, material science, and cell biology.

**KEYWORDS:** probe, charge transfer, dynamic mapping, liquid–solid interface, pixelated-TENG

## INTRODUCTION

Over the last ten years, a number of research groups have begun to explore the contact electrification (CE) and charge transfers between the liquid and solid interface,<sup>1–5</sup> and the related mechanisms have been widely discussed, such as the type of charge carriers (electron<sup>6–8</sup> or ion transfer<sup>9,10</sup>) and the formation of an electric-double layer (EDL).<sup>11–14</sup> The charge transfer at a liquid–solid interface is crucial for many fields, and examples range from energy harvesting (liquid–solid triboelectric nanogenerators)<sup>15–20</sup> to surface electrochemistry,<sup>9,21,22</sup> electrocatalysis,<sup>23,24</sup> and biochemistry. The role of the charge transfer at the liquid–solid interface should also be taken into consideration for the description of water moving on hydrophobic surfaces.<sup>25</sup> However, quantifying the charge transfer, especially for the in situ dynamic mapping of interface charge transfer at a liquid–solid contact is rather limited and still remains ambiguous due to the lack of fundamental detection technology.<sup>26</sup>

The droplet triboelectric nanogenerator (droplet-TENG), based on the contact electrification between liquid droplet and solid, is widely used in energy harvesting,<sup>16,18,20,27,28</sup> environ-



mental monitoring,<sup>29</sup> and biomedical sensors.<sup>30</sup> In recent years, our groups have started to measure the charge transfer at the liquid–solid interface with the droplet-TENG.<sup>14,16,31</sup> The water-TENG with a superhydrophobic micro-/nanostructured polytetrafluoroethylene was developed to harvest the water-related energy from flowing water, and by studying the relationship between the motion of a single water drop onto the water-TENG, a sequential contact-electrification and electrostatic-induction process is proposed to describe the working mechanism of the water-TENG.<sup>16</sup> Further, in 2020, we have developed the one-electrode water droplet-TENG, and by analyzing the electric information from multiple droplets contact and separate with a hydrophobic polymer

**Received:** November 21, 2022

**Accepted:** January 3, 2023

surface, we have shown that the droplet-TENG could be a promising probe for studying the charge transfer at liquid–solid interface.<sup>14</sup> Then the experiment was further improved in 2021.<sup>31</sup> In this work, a self-powered droplet-TENG with two separated electrodes was developed. By means of measuring the electric signal on spatially arranged electrodes, we showed that the charge transfer between droplets and solid is an accumulation process during the dropping and that the electron is the dominant charge-transfer species. However, the use of only one metallic electrode can only tell us the total transferred charges of the droplet along the entire path of the sliding route but fail to keep monitoring the charge transfer at the microscopic level. The water droplet-TENG with two parallel electrodes, can distinguish the difference in charge transfer at Y-axis (direction of droplet movement), while there is still limitation in resolving the charge transfer at X-axis direction. Moreover, neither of the above two types of water droplet-TENG can achieve high resolution of charge transfer mapping at both X and Y axis. Therefore, the in situ dynamic charge mapping of the movement trajectory of water droplet is at present still not accessible.

Herein, we have developed a pixelated droplet-TENG with spatially arranged high-density metallic electrode arrays at pixel size of 0.4 mm. The information of electric signal at each electrode provides the opportunity to probe the 2D high-resolution charge distribution when water drop moves on the hydrophobic solid surface. The effects of light intensity and pH value of the aqueous solutions on the charge transfer between liquid droplet and dielectric solid were also investigated. Our study reveals that the buildup of induced transferred charges does not uniformly distribute when the water drop moves on the tilted solid surface. An explanation based on the two-step model of electron and ion transfer is proposed, and thus, the formation of an electric double-layer (EDL) will shield the net surface charges on the solid surface. Most importantly, such pixelated droplet-TENG showing a high sensitivity to the water movement, pH, and light intensity, may therefore present as a promising probe for application in physical chemistry, surface chemistry, electrochemistry, catalysis, and biosensors.

## RESULT AND DISCUSSION

### Contact Electrification between a Water Droplet and a Tilted Fluorinated Ethylene Propylene (FEP) Surface.

The experimental setup is shown in Figure 1a. Here, the flat dielectric FEP film was attached on a poly(methyl methacrylate) (PMMA) plate. FEP was selected to be electrified with a water droplet due to the higher water contact angle and strong affinity to electrons (rich fluorine groups). The water droplet was released from a grounded needle by a syringe pump at a fixed height (0.8 cm) above the polymer surface at a vertical angle. When the water droplet flowed through the copper electrode array located under the FEP film, the surface induced charges on the FEP surface were measured at the same time, and thus, the in situ charge mapping can be obtained. Figure 1b shows the fabrication of the pixelated droplet-TENG, including three parts: the top layer is a dielectric FEP film for contact electrification with a liquid droplet, while the bottom part is signal processing to capture the electrostatic induction signal induced by charge transfer between the water droplet and FEP film. The middle part is a PMMA plate, and the Cu electrode array (a total of 432 individual copper electrodes distributed in 12 columns and 36 rows) penetrates the PMMA plate. The arrangement of the Cu

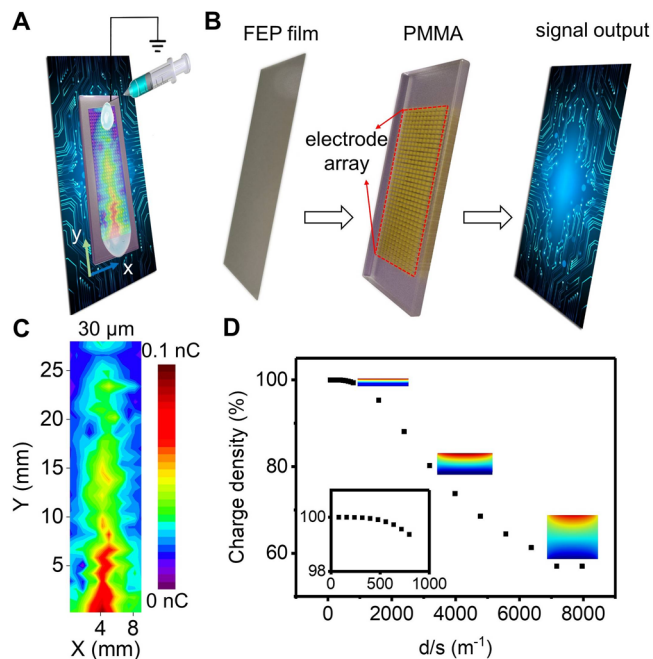


**Figure 1.** Experimental setup. (a) Working mechanism of the pixelated droplet-TENG. When a water droplet flows through the tilted fluorinated ethylene propylene surface, the charge transfer between liquid and solid occurred, and the induced charges at each point were measured by the electrode arrays on the backside. The *x*- and *y*-axes represent the direction of movement of the liquid droplet. (b) Structure of the pixelated droplet-TENG: the top layer is dielectric polymer film (FEP film) for contact electrification with water droplet; the middle layer is a PMMA plate, and the Cu electrode array (12 × 36 Cu electrodes) penetrates the PMMA plate; the bottom layer is a signal processor. (c) Two-dimensional induced surface charge mapping of a water droplet sliding through the FEP film (the thickness is 30 μm). (d) Simulation results of induced charges under different film thickness; *d* is the film thickness, and *s* is the area of a single Cu electrode.

electrode array on the X- and Y-axis is shown in Supplementary Figure 1. Therefore, one end of the Cu electrode array can be connected to the FEP film, while the other end is connected to the signal processor. In this way, each individual electrode in the array can be a probe for charge transfer, and thus, 432 separated probes are available for high-resolution induced transferred charge mapping in our pixelated droplet-TENG. Such a pixelated droplet-TENG with a high electrode density has high spatial resolution of 0.4 mm on both the X and Y axes compared to the single electrode droplet-TENG can provide abundant information on the charge transfer between the liquid droplet and dielectric solid, for example, the charge saturation point and the effect of sliding speed on the induced charge. The surface charge mapping can be obtained from the induced charges (calculation of induced charges is in Supplementary Figure 2) at each probe (Figure 1c). From Figure 1c, the induced charges recorded on each probe are surprisingly different, in other words, the induced charges are not uniformly distributed throughout the water droplet sliding on the tilted FEP surface. Our data show that at the X-axis across the droplet (the X- and Y-axes are shown in Figure 1a) the induced charges at the center part of the droplet are almost three times higher than that in the edge part at Y = 0.2 mm, see Supplementary Figure 3a. This is easy to understand and should be attributed to the poor contact (or no contact)

between the edge part of the water droplet and FEP surface. Very surprisingly for the Y-axis here, this value (the sum of the transferred charges for each row) gradually increases (from 0.25 to 0.62 nC) as the water droplet slides on the FEP surface (Supplementary Figure 3b). There is limited published data on charge transfer measurement at such a high-resolution probe, but our findings are in contrast to the papers published on solid/solid contact electrification: the transferred charges upon contact electrification should be the same within the same contact area.<sup>32</sup> Further, COMSOL Multiphysics (5.4 version) was used to study the induced charges at different ratios of thicknesses of FEP film and each electrode area ( $d/s$ ) (Figure 1d and Supplementary Figure 4). Here, the amount of transferred charges between the water droplet and FEP film is set to 100% and the electrode area is constant in all of our experiments. When the induced charges of different  $d/s$  are compared, what becomes apparent is that the induced charges generated by contact electrification between the liquid–solid interface scales with the thickness of FEP film. However, when the thickness of the FEP film is less than 50  $\mu\text{m}$ , that is, the  $d/s$  is less than 500, see Figure 1d, there is almost no difference between the induced charges and the surface charge transfer between the water droplet and FEP film. Therefore, the choice of a 30  $\mu\text{m}$  FEP film in our experiments is reasonable.

**Pixeled Droplet-TENG Probes the In Situ Dynamic Process of Water Drop Moves on the Hydrophobic Solid Surface.** In our experiment, the motion of a water droplet on the FEP surface was recorded by a fast camera, and the selected snapshots of a water droplet sliding across the tilted FEP surface (30°) at different times (0, 0.02, 0.04, 0.06, 0.08, 0.10, 0.12, 0.14, 0.16, and 0.18 s) are presented in Figure 2a. During the process of dropping, although the water droplet has been kept in contact with the FEP surface, its motion trajectory is very complicated. The lateral adhesion, the resistance of drops to sliding motion, viscous dissipation, and also the static charging<sup>25</sup> all needed to be considered for their effects on the motion trajectory of the droplet. For example, the water droplet shows different shapes at different times: the water droplet is spread to become conelike from 0 to 0.08 s, and then the water droplet is circular at 0.10 s and immediately followed with a rectangle (0.12 s) shape and then back to conelike (0.14 s) and starts to slide down on the surface until it is detached from the electrode array (Figure 2a). Contact electrification is closely related to the contact area, time, and interaction force between contacting materials. Thus, the state of the water droplet during the movement of the FEP surface will directly affect the charge transfer between the liquid–solid interface. In this way, our pixeled droplet-TENG could be a probe to measure the in situ dynamic process of water drop moves on the hydrophobic solid surface. The results in Figure 2b show evidence of it. The corresponding mappings of transferred charges at different dropping times are shown in Figure 2b, and viewed from the  $y$ -axis, we found that the induced charges increase as the water droplet moves on the FEP surface but suddenly decrease at some points, such as  $Y = 18.6, 19.4,$  and  $21.8$  mm, see Supplementary Figure 3b and Figure 2b. If the density of the electrodes is not sufficient, such as in the previously published work with only one or two electrodes,<sup>14,31</sup> these points will be mistaken for charge saturation points as the transferred charges decreased on these points. This finding carries a cautionary message on what to consider when measuring the charge transfer during water drop moves on the hydrophobic surface, especially for the

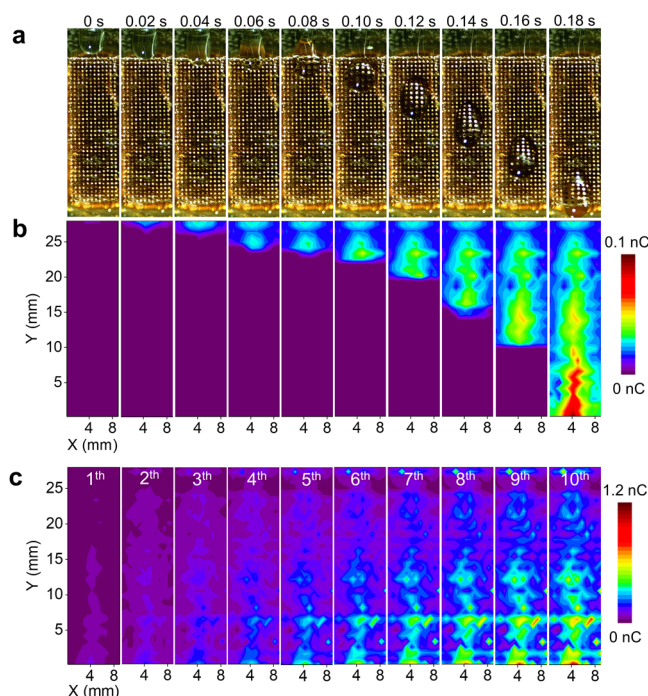


**Figure 2.** Time-resolved mappings of charge transfer between water droplet and FEP surface. (a) Snapshots showing the motion of a water droplet on the tilted FEP film at different times (0, 0.02, 0.04, 0.06, 0.08, 0.10, 0.12, 0.14, 0.16, and 0.18 s). The copper electrodes array ( $12 \times 36$ ) was located under the transparent FEP surface. (b) Corresponding time-resolved mappings of charge transfer between water droplet and FEP surface at different time. (c) Induced charge transfer mappings of contact electrification between the FEP film and continuous water droplets. Each mapping is the sum of the induced charges on all drops of water moving on the FEP surface, for example, the mapping of 10th droplet of water represents the sum of the induced charges generated by each drop (from 1th to 10th). Images from left to right are the induced charge of first to ten drops of water.

determination of the charge saturation point. The charge saturation phenomenon occurred in the process of the multiple droplets sliding on the dielectric solid surface. As the droplet number increased, the transferred charges measured on the polymer surface decreased until a saturation point was reached. This phenomenon is also probed by our pixeled droplet-TENG. The induced charge mappings from the interaction between a sequence of water droplets and tilted FEP films were measured by our pixeled droplet-TENG (Figure 2c). As the droplet number increased (from the first droplet to the 10th drop), the transferred charges between the FEP surface and water droplets decreased at each droplet (Supplementary Figure 5). Also, the mappings of transferred charges as a function of droplet number are shown in Figure 2c, and we found the transferred charges between water droplets and FEP is almost saturated when the ninth drop of water detached from the FEP surface (Supplementary Figure 5). The understanding of the phenomenon of charge saturation is very limited, and is not clear until now, which was thought to be that the charge saturation prevents further electron transfer between the liquid and solid. The above discussion proves that our pixeled droplet-TENG can compensate for the defects of the single-electrode droplet-TENG published in the previous work in detecting charge transfer at the liquid–solid interface, and such high-density pixeled droplet-TENG can probe the

charge transfer and saturation point more accurately and sensitively.

**Pixelated Droplet-TENG Probes the Effect of the Light Intensity on the CE between the Water Droplet and Solid Surface.** Electrons could be excited and emitted out of the dielectric surface under the excitation of ultraviolet photons, which is known as photoelectron emission. Thus, the light irradiation should be an effective way to release surface triboelectric charges.<sup>3</sup> Therefore, our pixelated droplet-TENG should be an effective probe to investigate the effect of the light on the charge transfer between the water droplet and solid surface. Here, we focus on the effects of the light's intensity on the transferred charges mapping (Figure 3a–c).

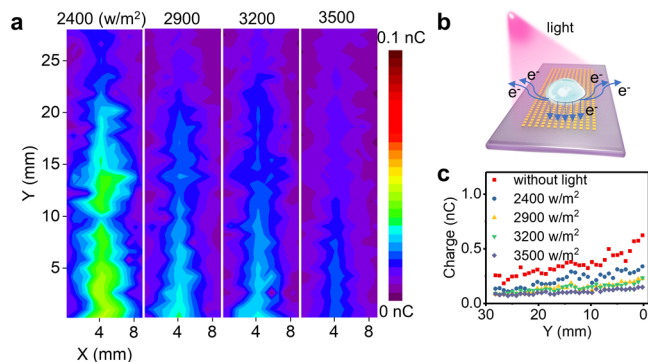


**Figure 3.** Effect of the light intensity on the induced charge mapping generated by CE between the water droplet and FEP film. (a) Induced transferred charge mappings of contact electrification between the FEP film and water droplet under different light intensities: 2400, 2900, 3200, and 3500  $\text{W}/\text{m}^2$ . (b) Schematic illustration of the light irradiation experiments. (c) Change of charge transfer in the Y-axis direction at different light intensities.

When the induced charge mapping for samples under different light intensities are compared, what becomes apparent is that the transferred charges generated by CE between the water droplet and FEP decreased with increasing light intensity (Figure 3a). The slope of the charge transfer development from the y-axis changed from 0.013 to 0.002  $\text{nC}/\text{mm}^{-1}$  when the light intensity varied from 0 to 3500  $\text{W}/\text{m}^2$  (Figure 3c), indicating that light irradiation is an efficient way to release surface charges on the liquid–solid interface. This result is consistent with the photoelectron emission theory of electrons, and this relationship further reinforces that the static charge carriers should be electrons. Figure 3b shows the schematic illustration of the light irradiation experiments. In the experiment, the light shines directly on the FEP surface and the wavelength of the light remains unchanged, thus, the energy of the incident photons was kept constant, and the probability of the electrons being excited also remained unchanged in the experiments. It is already known that when the water droplet moves on the FEP film, the electrons will transfer from the water droplet to the FEP film as FEP has a strong affinity to electrons<sup>14</sup> (Figure 3b), thus, the water droplet becomes positively charged, while the FEP film will be negatively charged. Therefore, when the light intensity increased, the number of incident photons and excited electrons per unit time increased, resulting in some residual electrons on the FEP surface being excited and thus decreasing the net charges on the FEP interface (Figure 3b).

### Pixelated Droplet-TENG Probes the Liquid pH Value on the CE between the Water Droplet and Solid Surface.

Further, the effects of the pH value of the liquid droplet on the charge transfer between the liquid–solid interface were studied. The CE between the FEP film and different aqueous solutions, including HCl and NaOH solutions with different pH values, were performed in our experiment, and the transferred charge mappings were recorded in Figure 4a. As

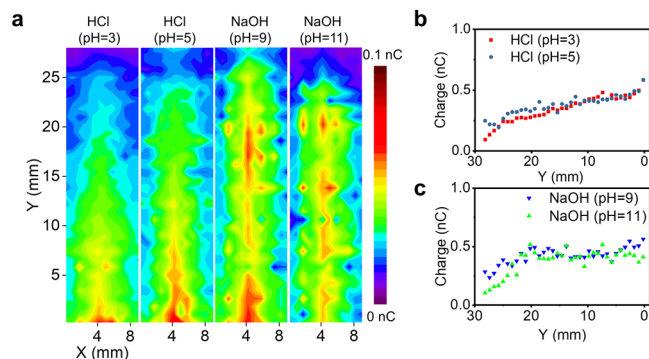


**Figure 4.** Effect of the pH value on the induced charge mapping generated by CE between the water droplet and FEP film. (a) Induced charge transfer mappings of contact electrification between FEP film with different droplets: HCl (pH = 3), HCl (pH = 5), NaOH (pH = 9), and NaOH (pH = 11). (b) Development of the transferred charges on the Y-axis when a droplet of HCl (pH = 3 and pH = 5) moves on the surface of a FEP film. (c) Development of the transferred charges on the Y-axis when a droplet of NaOH (pH = 9 and pH = 11) moves on the surface of a FEP film.

seen from Figure 4a,b, the trend of the transferred charge development of acid droplets on the y-axis is similar to that of water droplets, thus leading to the similar shape of transferred charge mappings (the transferred charges continue to increase with the acid droplet motion). However, when the base droplet, here is NaOH drop, moves on the FEP surface, the shape of the transferred charge mapping changed. The transferred charges look more uniform throughout the whole process of the NaOH droplet sliding on the FEP surface, especially when the pH of NaOH is 9 (the transferred charges increase with droplet motion until  $y$  is 20 mm, and then the transferred charges remain constant in Figure 4c). Therefore, the shape of transferred charges mapping can be used as an indicator to distinguish acidity and alkalinity by our pixelated droplet-TENG.

The existence of EDL and its structure is well understood, a fundamental question is the cause of the first layer becoming charged at the very beginning when it first contacts with a liquid. This question was addressed by the “two-step” model proposed by Wang et al.,<sup>13</sup> and the “two-step” model has also been proved by our experiments. In the first step, when the liquid drop contacts a fresh FEP surface (Figure 5), the electrons will transfer from the water molecules to solid atoms due to the overlap of the electron clouds of water molecules and solid atoms,<sup>11</sup> resulting in the positively charged water and negatively charged FEP surface. In the second step, for the opposite ions, the cations in the droplet would move to the negatively charged FEP surface due to the electrostatic interactions, thus forming an EDL at the liquid–solid interface. In this way, the adsorption of ions on the solid surface and thus the formation of the EDL will inevitably shield the net surface

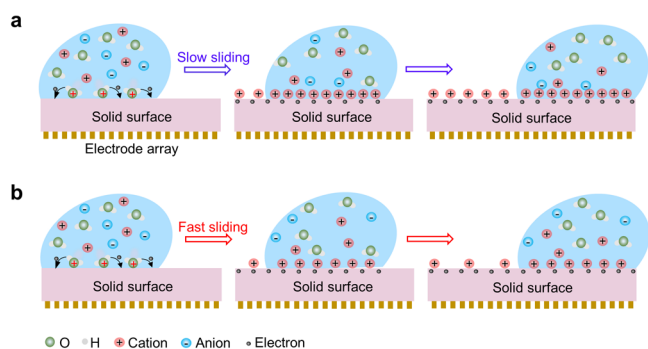


**Figure 5.** Mechanism of the pixelated droplet-TENG. (a) The liquid droplet moves on a FEP surface at slow sliding rate. The electron transfer occurred first, and when the sliding rate is slow, more cations adsorbed on the FEP surface. (b) The liquid droplet moves on a FEP surface at a fast sliding rate, leading to the less adsorbed cations on the FEP surface.

charges on the solid surface. For example, fewer the ions are absorbed on the hydrophobic surface than on the hydrophilic surface, and the transferred charges generated between a liquid droplet and hydrophobic surface are much higher than those of the hydrophilic surface.<sup>11</sup> Therefore, the longer the CE time between liquid and solid, the more ions adsorbed on the solid surface, and thus the stronger shielding effect should be observed. In our experiment, the liquid droplet movement on the tilted FEP surface is an accelerated movement due to the gravity of droplet. Thus, the time required for the liquid droplet to flow through each electrode is different: the droplet is moving slow at the beginning and then gradually accelerating. When the liquid drop moves slowly across the electrode, more cations are adsorbed on the FEP surface to form EDL (Figure 5a), resulting in a strong shielding effect and the reduction of the net charges on the FEP surface. On the contrary, the fast sliding of the droplet leads to fewer cations being adsorbed on the FEP surface and thus detection of higher net charges (Figure 5b). To further prove this hypothesis, we have performed the experiment at a tilted angle of FEP at 45°, and under this condition, the droplet slides down at a slower rate, thus, the decreased transferred charges should be observed. As expected, the reduction in the amount of transferred charges confirms our mechanism (Supplementary Figure 6). We also note that the droplet thickness had no measurable effect on transferred charges (Supplementary Figure 7). The effect of the pH values can also be explained: as the number of cations increases in the droplet, for example, more H<sup>+</sup> adsorbed on the charged FEP surface, leading to a decrease of net charges on FEP measured for acid solution. On the other hand, for NaOH solution (decreased H<sup>+</sup> and increased Na<sup>+</sup>), Na<sup>+</sup> moves slower due to its large ion diameter compared with H<sup>+</sup> and therefore needs more time to form the EDL. This should be the reason for the uniform distribution of charge mapping for NaOH. Further, as water droplets continue to flow through the FEP surface, more H<sup>+</sup> accumulate on the surface to form an EDL, which shields the net charges on the FEP surface. This is probably a possible explanation for charge saturation phenomenon.

## CONCLUSION

In this work, we have developed a pixelated droplet-TENG with an electrode array as a probe for in situ dynamic mapping of interface charge transfer at liquid–solid contact. Such

transferred charge mapping shows high sensitivity to the movement of the droplet, light intensity, and pH values of liquid. From the increasing/decreasing of the transferred charges in the mapping or the shape changing of the mapping, we can not only obtain the physical or chemical information on the contacting materials, including liquid droplet and the contact solid film, but also the dynamic information on the droplet movement, such as velocity and acceleration. Further, our conclusions support the “two-step” model about the formation of EDL, in which the electron transfer at the first step and then the ions adsorbed are verified experimentally. Practically, the work shows that the use of pixel droplet-TENG may provide a method to measure the microscopic charge transfer beyond AFM experiments. Therefore, our pixelated droplet-TENG has implications for detection of surface properties (chemical and physical properties) of materials, chemical sensing, and biomedical sensors and also would help refine the description of forces acting on the moving droplet.

## METHODS

**Materials.** Redistilled solvents and Milli-Q water (>18 MΩ cm) were used for substrate cleaning and to prepare solutions. Films of fluorinated ethylene propylene (FEP, 30 μm, DAIKIN) were used for contact with the liquid droplet. Hydrochloric acid (37%) and sodium chloride (99%) were purchased from Sigma.

**Fabrication of Pixel-TENG.** The copper electrode array was composed of 432 (12 × 36) individual electrodes with a diameter of 0.4 mm on a smooth and clean poly(methyl methacrylate) (PMMA) plate (5 × 10 × 0.5 cm<sup>3</sup>), and a PMMA plate was used as the backboard. The shape of the copper electrode is round, and the area for each electrode is 0.12 mm<sup>2</sup>. We used Cu wire with insulated varnish covered on as both the electrode and wire. One end of the copper wire is polished to form a round copper electrode. We have removed the varnish at 1 cm from another end of the copper wire, so that this conductive part can be connected to the electrometer, thus, each electrode can be connected to the different channels of electrometer independently. The distance between the electrodes is 0.4 mm. The FEP films were carefully attached on the PMMA plate. FEP films were extensively washed with ethanol prior to each experiment to remove static charges.

**Electrical Measurements.** The copper electrode arrays on the PMMA plate were connected to National Instruments NI PXLe-1075 electrometers. The NI PXLe-1075 electrometers with a Labview program on a computer were used to measure the electric signal on each copper electrode produced by the interaction between the droplet and the FEP. In all experiments, the volume of liquid droplet is 55 μL per drop, the droplet height was set as 0.8 cm, the air humidity was 35%, and the temperature was 24 °C. The liquid droplet was dripped by a syringe pump (PHD ULTRA Series, Harvard apparatus) and was grounded in the experiment. The photos were captured by high-speed camera (Photron, FSATCAM Mini AX). The distance between the light device (Newport 67005) and droplet-TENG is 6 cm.

## ASSOCIATED CONTENT

### Supporting Information

The Supporting Information is available free of charge at <https://pubs.acs.org/doi/10.1021/acsnano.2c11633>.

Additional arrangement of the Cu electrode array, calculation of the transferred surface charge at each electrode, the development of the transferred charge on the *x* and *y* axes, the simulation model used for studying the induced charge under different film thickness, and the induced transferred charge mappings at titled angle of 45° and 60° (PDF)

## AUTHOR INFORMATION

## Corresponding Author

Zhong Lin Wang – Beijing Institute of Nanoenergy and Nanosystems, Chinese Academy of Sciences, Beijing 100083, P.R. China; School of Nanoscience and Technology, University of Chinese Academy of Sciences, Beijing 100049, P.R. China; School of Materials Science and Engineering, Georgia Institute of Technology, Atlanta, Georgia 30332-0245, United States; [orcid.org/0000-0002-5530-0380](https://orcid.org/0000-0002-5530-0380); Email: [zlwang@gatech.edu](mailto:zlwang@gatech.edu)

## Authors

Jinyang Zhang – Beijing Institute of Nanoenergy and Nanosystems, Chinese Academy of Sciences, Beijing 100083, P.R. China; School of Nanoscience and Technology, University of Chinese Academy of Sciences, Beijing 100049, P.R. China

Shiquan Lin – Beijing Institute of Nanoenergy and Nanosystems, Chinese Academy of Sciences, Beijing 100083, P.R. China; School of Nanoscience and Technology, University of Chinese Academy of Sciences, Beijing 100049, P.R. China

Complete contact information is available at:  
<https://pubs.acs.org/10.1021/acsnano.2c11633>

## Author Contributions

#J.Z. and S.L. contributed equally to this work.

## Notes

The authors declare no competing financial interest.

## ACKNOWLEDGMENTS

This research was supported by the National Natural Science Foundation of China (Grant Nos. 22102010 and 52005044) and the National Key R&D Project from Minister of Science and Technology (2021YFA1201601).

## REFERENCES

- (1) Li, X.; Zhang, L.; Feng, Y.; Zhang, X.; Wang, D.; Zhou, F. Solid–Liquid Triboelectrification Control and Antistatic Materials Design Based on Interface Wettability Control. *Adv. Funct. Mater.* **2019**, *29* (35), 1903587.
- (2) Lin, S.; Zhu, L.; Tang, Z.; Wang, Z. L. Spin-selected electron transfer in liquid–solid contact electrification. *Nat. Commun.* **2022**, *13* (1), 5230.
- (3) Lin, S.; Xu, L.; Zhu, L.; Chen, X.; Wang, Z. L. Electron transfer in nanoscale contact electrification: photon excitation effect. *Adv. Mater.* **2019**, *31* (27), 1901418.
- (4) Nie, J.; Ren, Z.; Xu, L.; Lin, S.; Zhan, F.; Chen, X.; Wang, Z. L. Probing Contact-Electrification-Induced Electron and Ion Transfers at a Liquid–Solid Interface. *Adv. Mater.* **2020**, *32* (2), 1905696.
- (5) Shahzad, A.; Wijewardhana, K. R.; Song, J.-K. Contact Electrification Efficiency Dependence on Surface Energy at the Water–Solid Interface. *Appl. Phys. Lett.* **2018**, *113* (2), 023901.
- (6) Gibson, H. W. Linear free energy relations. V. Triboelectric charging of organic solids. *J. Am. Chem. Soc.* **1975**, *97* (13), 3832–3833.
- (7) Byun, K.-E.; Cho, Y.; Seol, M.; Kim, S.; Kim, S.-W.; Shin, H.-J.; Park, S.; Hwang, S. Control of Triboelectrification by Engineering Surface Dipole and Surface Electronic State. *Adv. Mater. Interfaces* **2016**, *8* (28), 18519–18525.
- (8) Liu, C.-y.; Bard, A. J. Electrons on Dielectrics and Contact Electrification. *Chem. Phys. Lett.* **2009**, *480* (4–6), 145–156.
- (9) Zhang, J.; Rogers, F.; Darwish, N.; Gonçalves, V. R.; Vogel, Y. B.; Wang, F.; Gooding, J. J.; Peiris, M. C.; Jia, G.; Veder, J.-P.; Coote, M. L.; Ciampi, S. Electrochemistry on Tribocharged Polymers is Governed by the Stability of Surface Charges Rather than Charging Magnitude. *J. Am. Chem. Soc.* **2019**, *141*, 5863–5870.
- (10) McCarty, L. S.; Whitesides, G. M. Electrostatic charging due to separation of ions at interfaces: contact electrification of ionic electrets. *Angew. Chem., Int. Ed.* **2008**, *47* (12), 2188–2207.
- (11) Lin, S.; Xu, L.; Wang, A. C.; Wang, Z. L. Quantifying Electron-Transfer in Liquid–Solid Contact Electrification and the Formation of Electric Double-Layer. *Nat. Commun.* **2020**, *11* (1), 1–8.
- (12) Moon, J. K.; Jeong, J.; Lee, D.; Pak, H. K. Electrical Power Generation by Mechanically Modulating Electrical Double Layers. *Nat. Commun.* **2013**, *4* (1), 1–6.
- (13) Wang, Z. L.; Wang, A. C. On the origin of contact-electrification. *Mater. Today* **2019**, *30*, 34–51.
- (14) Zhan, F.; Wang, A. C.; Xu, L.; Lin, S.; Shao, J.; Chen, X.; Wang, Z. L. Electron Transfer as a Liquid Droplet Contacting a Polymer Surface. *ACS Nano* **2020**, *14* (12), 17565–17573.
- (15) Tang, W.; Chen, B. D.; Wang, Z. L. Recent Progress in Power Generation from Water/Liquid Droplet Interaction with Solid Surfaces. *Adv. Funct. Mater.* **2019**, *29* (41), 1901069.
- (16) Lin, Z. H.; Cheng, G.; Lee, S.; Pradel, K. C.; Wang, Z. L. Harvesting water drop energy by a sequential contact-electrification and electrostatic-induction process. *Adv. Mater.* **2014**, *26* (27), 4690–4696.
- (17) Liu, Y.; Zheng, Y.; Li, T.; Wang, D.; Zhou, F. Water–Solid Triboelectrification with Self-Repairable Surfaces for Water-Flow Energy Harvesting. *Nano Energy* **2019**, *61*, 454–461.
- (18) Xu, W.; Zheng, H.; Liu, Y.; Zhou, X.; Zhang, C.; Song, Y.; Deng, X.; Leung, M.; Yang, Z.; Xu, R. X. A droplet-based electricity generator with high instantaneous power density. *Nature* **2020**, *578* (7795), 392–396.
- (19) Yin, J.; Zhang, Z.; Li, X.; Zhou, J.; Guo, W. Harvesting Energy from Water Flow over Graphene? *Nano Lett.* **2012**, *12* (3), 1736–1741.
- (20) Zhong, W.; Xu, L.; Zhan, F.; Wang, H.; Wang, F.; Wang, Z. L. Dripping Channel Based Liquid Triboelectric Nanogenerators for Energy Harvesting and Sensing. *ACS Nano* **2020**, *14* (8), 10510–10517.
- (21) Lee, J. K.; Walker, K. L.; Han, H. S.; Kang, J.; Prinz, F. B.; Waymouth, R. M.; Nam, H. G.; Zare, R. N. Spontaneous generation of hydrogen peroxide from aqueous microdroplets. *Proc. Natl. Acad. Sci. U. S. A.* **2019**, *116* (39), 19294–19298.
- (22) Song, X.; Meng, Y.; Zare, R. N. Spraying Water Microdroplets Containing 1, 2, 3-Triazole Converts Carbon Dioxide into Formic Acid. *J. Am. Chem. Soc.* **2022**, *144* (37), 16744–16748.
- (23) Wang, Z.; Berbille, A.; Feng, Y.; Li, S.; Zhu, L.; Tang, W.; Wang, Z. L. Contact-electro-catalysis for the degradation of organic pollutants using pristine dielectric powders. *Nat. Commun.* **2022**, *13* (1), 1–9.
- (24) Zhang, J.; Lin, S.; Wang, Z. L. Electrostatic Charges Regulate Chemiluminescence by Electron Transfer at the Liquid–Solid Interface. *J. Phys. Chem. B* **2022**, *126* (14), 2754–2760.
- (25) Li, X.; Bista, P.; Stetten, A. Z.; Bonart, H.; Schür, M. T.; Hardt, S.; Bodziony, F.; Marschall, H.; Saal, A.; Deng, X. Spontaneous charging affects the motion of sliding drops. *Nat. Phys.* **2022**, *18*, 713–719.
- (26) Zhang, J.; Coote, M. L.; Ciampi, S. Electrostatics and Electrochemistry: Mechanism and Scope of Charge-Transfer Reactions on the Surface of Tribocharged Insulators. *J. Am. Chem. Soc.* **2021**, *143* (8), 3019–3032.
- (27) Helseth, L. E. A water droplet-powered sensor based on charge transfer to a flow-through front surface electrode. *Nano Energy* **2020**, *73*, 104809.
- (28) Wu, H.; Mendel, N.; van den Ende, D.; Zhou, G.; Mugele, F. Energy harvesting from drops impacting onto charged surfaces. *Phys. Rev. Lett.* **2020**, *125* (7), 078301.
- (29) Zhou, Z.; Li, X.; Wu, Y.; Zhang, H.; Lin, Z.; Meng, K.; Lin, Z.; He, Q.; Sun, C.; Yang, J. Wireless self-powered sensor networks driven by triboelectric nanogenerator for in-situ real time survey of environmental monitoring. *Nano Energy* **2018**, *53*, 501–507.

(30) Lai, Y. C.; Deng, J.; Zhang, S. L.; Niu, S.; Guo, H.; Wang, Z. L. Single-thread-based wearable and highly stretchable triboelectric nanogenerators and their applications in cloth-based self-powered human-interactive and biomedical sensing. *Adv. Funct. Mater.* **2017**, *27* (1), 1604462.

(31) Zhang, J.; Lin, S.; Zheng, M.; Wang, Z. L. Triboelectric Nanogenerator as a Probe for Measuring the Charge Transfer between Liquid and Solid Surfaces. *ACS Nano* **2021**, *15* (9), 14830–14837.

(32) Zhang, J.; Ferrie, S.; Zhang, S.; Vogel, Y. B.; Peiris, C.; Darwish, N.; Ciampi, S. Single-Electrode Electrochemistry: Chemically Engineering Surface Adhesion and Hardness to Maximize Redox Work Extracted from Tribocharged Silicon. *ACS Appl. Nano Mater.* **2019**, *2*, 7230–7236.